●5● おわりに ●●●

医工連携さらには産学連携による技術革新，産業創出が叫ばれて久しい。政府の支援を受けてさまざまなプロジェクトが立ち上げられてきたが，いわゆる成功例は数えるほどしかないのが現状である。本章の「医用画像による骨関節形態および動態解析・予測」は産業界で製作されるCTやMRI装置という診断機器が急速に進歩を遂げている一方で，医師サイドからは骨関節3次元動態を評価して治療したいというニーズは満足されていないという実情があったが，その間を工学系の情報，画像処理技術が埋めることによってすばらしい治療体系が広がろうとしている。そういう意味では本章内で紹介された技術は医工，産学連携の大成功例といえるだろう。また未来の治療への可能性を示唆するといった不確定なものではなく，すでにいくつかの医療施設では今週，来週の手術治療に用いられている。

しかるに，革新的な治療体系の門戸がようやく開かれたばかりであり，今後解決しなければならない問題点も山積している。しかし問題点に関しては，難破船が大海で進路がわからずに迷走するようなものではなく，問題点の方向性は明確である。それを多くの優秀な医・工・情報学系研究者が一つ一つ解決し，さらなる治療体系の革新に繋がることが望まれる。

今後高齢化社会のさらなる加速に伴ってニーズも加速度的に増大することが予想される。また骨関節のいわゆる整形外科領域だけでなく他の診療科でのニーズも汲んでいくことによって，研究領域も拡大していくものと思われる。さまざまな技術，研究を行っている医・工・情報学系研究者にとって，それが世の中でなんの役に立とうとしているかが，ややもすると曖昧になることがある。しかし悩める患者の治療に役立つという最も直接的な貢献を体感することは研究者冥利につきることである。多くの若手研究者が参画し，さまざまな分野で革新的な治療が広げられることを切望してやまない。

参考文献

(1) Lemieux, L *et al.* A patient-to-computed-tomography image registration method based on digitally reconstructed radiographs. *Med. Phys.* 21, 1749-1760 (1994)
(2) Murphy, MJ. An automatic six-degree-of-freedom image registration algorithm for image-guided frameless stereotaxic radiosurgery. *Med. Phys.* 24, 857-866 (1997)
(3) Weese J *et al.* Voxel-based 2-D/3-D registration of fluoroscopy images and CT scans for image-guided surgery. *IEEE Trans Inform. Technol. Biomed.* 1, 248-293 (1997)
(4) Hipwell JH. *et al.* Intensity-based 2-D－3-D registration of cerebral angiograms. *IEEE Trans. Med. Imag.* 22, 1417-1426 (2003)
(5) Banks, SA, Hodge, WA. Accurate measurement of three-dimensional knee replacement kinematics using single-plane fluoroscopy. *IEEE Trans. Biomed. Eng.* 43, 638-649 (1996)
(6) Hoff, WA. *et al.* Three-dimensional determination of femoral-tibial contact position under in-vivo conditions using fluoroscopy. *Clinical Biomech.* 13, 455-472 (1998)
(7) Zuffi, S. *et al.* A model-based method for the reconstruction of total knee replacement kinematics. *IEEE Trans. Med. Imag.* 18, 981-991 (1999)
(8) Mahfouz, MR. *et al.* A robust method for registration of three-dimensional knee implant models to two-

dimensional fluoroscopy images. *IEEE Trans. Med. Imag.* 22, 1561-1574 (2003)
(9) Yamazaki, T. *et al.* Improvement of depth position in 2-D/3-D registration of knee implants using single-plane fluoroscopy. *IEEE Trans. Med. Imag.* 23, 602-612 (2004)
(10) Weng, J. *et al.* Camera calibration with distortion models and accuracy evaluation. *IEEE Trans. Pattern. Anal. Mach. Intell.* 14, 965-980 (1992)
(11) Besl, PJ. and McKay, ND. A method for registration of 3-D shapes. *IEEE Trans. Pattern. Anal. Mach. Intell.* 14, 239-256 (1992)
(12) Lemieux, L. *et al.* Voxel based localization in frame-based and frameless stereotaxy and its accuracy. *Med. Phys.* 21, 1301-1310 (1994)
(13) Woods, RP. *et al.* MRI-PET registration with automated algorithm. *J. Comput. Assist. Tomogr.* 17, 536-546 (1993)
(14) Maes, F. *et al.* Multimodality image registration by maximization of mutual information. *IEEE Trans. Med. Imag.* 16,187-198 (1997)
(15) Holden, M. *et al.* Voxel similarity measures for 3-D serial MR brain image registration. IEEE Trans, Med. Imag. 19, 94-102 (2000)
(16) 松野誠夫ら『人工膝関節置換術―基礎と臨床―』文光堂，東京436-485 (2005)
(17) Tamaki M. *et al. In vivo* kinematic analysis of a high-flexion posterior stabilized fixed-bearing knee prosthesis in deep knee-bending motion. *J. Arthroplasty* 23, 879-885 (2008)
(18) Cates, HE. *et al. In vivo* comparison of knee kinematics for subjects having either a posterior stabilized or cruciate retaining high-flexion total knee arthroplasty. *J. Arthroplasty* 23, 1057-1067 (2008)
(19) Chouteau, J. *et al.* Kinematics of a cementless mobile bearing posterior cruciate ligament-retaining total knee arthroplasty. *Knee* 16, 223-227 (2009)
(20) Beggs, J. S. Kinematics. Washington: Hemisphere Publishing, 33-51 (1983)

Spine

SPINE Volume 36, Number 10, pp 778–783

BIOMECHANICS

In Vivo Three-Dimensional Kinematics of the Cervical Spine During Head Rotation in Patients With Cervical Spondylosis

Yukitaka Nagamoto, MD,* Takahiro Ishii, MD, PhD,† Hironobu Sakaura, MD, PhD,‡ Motoki Iwasaki, MD, PhD,‡ Hisao Moritomo, MD, PhD,‡ Masafumi Kashii, MD, PhD,§ Takako Hattori, MD,* Hideki Yoshikawa, MD, PhD,‡ and Kazuomi Sugamoto, MD, PhD*

Study Design. Kinematics of the cervical spine during head rotation was investigated using 3-dimensional (3D) magnetic resonance imaging (MRI) in patients with cervical spondylosis (CS).

Objective. To demonstrate *in vivo* 3D kinematics of the spondylotic cervical spine during head rotation.

Summary of Background Data. Several *in vivo* studies have identified kinematic differences between normal and spondylotic subjects, but only two-dimensional flexion/extension motion has been investigated. Differences of *in vivo* 3D cervical motion during head rotation between normal and spondylotic subjects have yet to be clarified.

Methods. Ten healthy volunteers (control group) and 15 patients with CS (CS group) underwent 3D MRI of the cervical spine with the head rotated to 5 positions (neutral, ±45° and ±maximal head rotation). Relative motions of the cervical spine were calculated by automatically superimposing a segmented 3D MRI of the vertebra in the neutral position over images for each position using volume registration. The 3D motions of adjacent vertebra were represented with 6 degrees of freedom by Euler angles and translations on the coordinate system.

Results. Compared with the control group, the CS group showed significantly decreased mean axial rotation and mean coupled lateral bending at C5–C6 and C6–C7 and significantly increased mean coupled lateral bending at C2–C3 and C3–C4, although both the groups showed the same pattern of coupled motions.

Conclusion. The *in vivo* 3D kinematics of the spondylotic cervical spine during head rotation was accurately depicted and compared with those of healthy cervical spines for the first time.

Key words: kinematics, coupled motion, cervical spondylosis, volume registration. **Spine 2011;36:778–783**

The human cervical spine is composed of highly specific tissues and structures, which together provide the extensive range of motion and considerable load-carrying capacity required for physical activities of daily living (ADL). This is 1 reason why degenerative changes in the cervical spine start as early as middle age and affect more than 95% of patients older than 65 years.[1] Even though nerve root or cord compression develops in 10% to 15% of the population,[2] the pathophysiology of cervical spondylosis (CS) remains poorly understood.[3]

Achieving a better understanding of this pathophysiology requires clarification of the differences in kinematics between the normal and spondylotic cervical spine. Several kinematic studies associated with aging and/or degeneration of the cervical spine have been reported using simple extension and flexion radiography,[4–7] motion analysis,[8] cineradiography,[9] and magnetic resonance imaging (MRI).[10] However, most of these studies have investigated only 2-dimensional flexion/extension motion, and 3-dimensional (3D) analysis using a motion analyzer has been vague and indirect. No study comparing in vivo 3D cervical motion during head rotation between normal and spondylotic subjects has been conducted, despite the importance of these motions in ADL. This is because of the difficulty in measuring *in vivo* cervical segmental motion, particularly during head rotation and lateral bending, which involves complex 3D motions called "coupled motion." We have developed a 3D MRI system to evaluate the *in vivo* 3D kinematics of the spine[11–14] and have already reported accurate *in vivo* 3D kinematics of the normal cervical spine using this method.[11–13] The objectives of this study were to investigate *in vivo* 3D kinematics of the spondylotic cervical spine during head rotation and to compare those with kinematics of the healthy cervical spine.

From the *Department of Orthopaedic Biomaterial Science Osaka University Graduate School of Medicine; †Department of Orthopaedic Surgery, Kaizuka City Hospital, Kaizuka; ‡Department of Orthopaedics, Osaka University Graduate School of Medicine; and §Department of Orthopaedic Surgery, Toyonaka Municipal Hospital, Shibahara, Toyonaka, Osaka, Japan.

Acknowledgment date: October 28, 2009. Revision date: March 13, 2009. Acceptance date: March 18, 2010.

The manuscript submitted does not contain information about medical device(s)/drug(s).

No funds were received in support of this work. No benefits in any form have been or will be received from a commercial party related directly or indirectly to the subject of this manuscript.

This study was approved by IRB of our institute.

Address correspondence and reprint requests to Yukitaka Nagamoto, MD, Department of Orthopaedic Biomaterial Science, Osaka University Graduate School of Medicine, 2-2 Yamadaoka, Suita, Osaka 5650871, Japan; E-mail: 7gam0to@gmail.com

DOI: 10.1097/BRS.0b013e3181e218cb

MATERIALS AND METHODS

Subjects in this study comprised 10 healthy volunteers (control group) and 15 patients with CS (CS group). The 10 healthy volunteers (5 men, 5 women; mean age, 25.1 years; range, 22–31 years) had neither neck pain nor any medical history of cervical spine disorders. As for the control group, all subjects were included in our previous publications[11–13] and retrospective analysis was performed. The 15 patients (7 men, 8 women; mean age, 60.2 years; range, 41–70 years) had been referred to our institution because of axial and/or neurologic symptoms and showed radiographic findings of CS as follows: loss of disc space height; spondylotic bars; foraminal osteophytes; and kyphosis. Subjects with a history of cervical spine surgery, trauma, tumors, infection, rheumatoid arthritis, or ossification of the posterior longitudinal ligament were excluded. All study protocols were approved in advance by the institutional review board.

Each subject was placed supine on the MRI table and underwent 3D MRI in 5 positions with the head rotated 0° (neutral position), 45°, and maximally to the left and right. All subjects were instructed to rotate the head as perpendicular as possible to the axis of the body trunk, and the shoulders were fixed to the table with a band. In the control group, MRI was performed using a 1.0-T commercial magnetic resonance system (Signa LX; General Electric, Milwaukee, WI). A 3D fast-gradient recalled acquisition in the steady state sequence was used with the following settings: repetition time, 8.0 ms; echo time, 3.3 ms; slice thickness, 1.5 mm; no interslice gap; flip angle, 10°; field of view, 24 cm; and 256 × 224 in-plane acquisition matrix. In the CS group, MRI was performed using a 1.5-T commercial magnetic resonance system (MAGNETOM Espree; Siemens, Erlangen, German). A 3D multiecho data imaging combination sequence was used with the following settings: repetition time, 40.0 ms; echo time, 20.0 ms; slice thickness, 1.3 mm; no interslice gap; flip angle, 12°; field of view, 24 cm; and 256 × 226 in-plane acquisition matrix. All subjects provided informed consent to undergo 3D MRI for the kinematics study and those for whom MRI proved difficult to perform because of axial and/or neurologic symptoms were excluded. All examinations were performed by the first or second author.

MRI data were saved in Digital Imaging and Communications in Medicine format and transmitted to a computer workstation, where image processing was performed using software developed in our laboratory (Virtual Place M series; Medical Imaging Laboratory, Tokyo, Japan). The method used in this study has been fully described in previous reports[11–13] and is, therefore, only described briefly here. This method showed high accuracy as follows: 0.24° for flexion/extension, 0.31° for lateral bending, 0.43° for axial rotation, 0.52 mm for superoinferior translation, 0.51 mm for anteroposterior translation, and 0.41 mm for lateral translation.[11] As a result of image processing (volume registration method), 3D motions of each vertebra expressed as a matrix were obtained. For easier comprehension of complicated 3D motions, relative 3D cervical motions of all motion segments were calculated by converting the matrix obtained by image processing into a matrix representing relative motion with respect to the inferior adjacent vertebra, and these motions were expressed in 6 degrees of freedom by Euler angles with the sequence of yaw (X)-pitch (Y)-roll (Z) and translations using a previously defined coordinate system as follows: the z-axis of occipital bone (Oc) was parallel to the line connecting anterior and posterior borders of the foramen magnum, with anterior considered positive. The y-axis was defined as perpendicular to the z-axis, with superior being positive. The x-axis was positive to the left. The coordinate system of C1 was defined using 2 points: the posteroinferior border of the anterior arch and the anteroinferior border of the posterior arch. Origins were located at the anterior border of the foramen magnum on Oc and the posteroinferior border of the anterior arch on C1. The coordinate system of subaxial cervical vertebrae was defined as follows: the origin was located at the most inferior point on the posterior wall of the vertebral body in the midsagittal plane. The z-axis was defined as the line connecting anterior and posterior points in the inferior plane of the vertebral body, with anterior considered positive. The y-axis was defined as perpendicular to the z-axis, with superior being positive. The positive x-axis was directed to the left (Figure 1).[11–13] The coordinate system was always set with moving vertebrae (suprajacent vertebra of the functional spinal unit) in this study. Mean values and standard

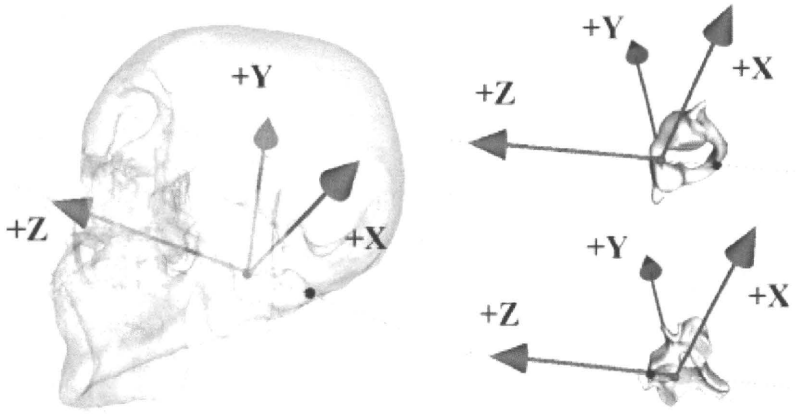

Figure 1. Anatomic orthogonal coordinate system for Oc, C1, and subaxial cervical vertebrae (C5). The methods have been fully described in previous studies.

TABLE 1. Rotations by Spinal Level for Control and CS Groups at 45° Head Rotation

	Oc–C1	C1–C2	C2–C3	C3–C4	C4–C5	C5–C6	C6–C7	C7–T1
AR								
Control(°)	0.4 ± 2.1	29.4 ± 3.2	0.5 ± 0.4	2.1 ± 0.5	2.4 ± 0.9	2.6 ± 0.7*	1.6 ± 0.7*	0.8 ± 0.6
CS(°)	0.2 ± 1.1	28.8 ± 3.7	0.9 ± 0.5	2.0 ± 0.7	2.0 ± 0.8	1.1 ± 0.7*	0.6 ± 0.3*	0.7 ± 0.3
Cp LB								
Control(°)	−4.0 ± 1.4*	−3.8 ± 1.8†	0.7 ± 1.2*	2.7 ± 0.7†	3.1 ± 0.8	2.8 ± 1.1*	2.5 ± 1.6†	0.5 ± 0.9
CS(°)	−2.3 ± 0.8*	−5.7 ± 1.6†	2.2 ± 1.0*	3.8 ± 1.2†	2.5 ± 1.3	1.3 ± 0.9*	1.3 ± 0.9†	0.6 ± 0.6
Cp F/E								
Control(°)	−5.4 ± 2.7†	−3.4 ± 2.0	−0.6 ± 1.0	0.8 ± 1.2	−1.1 ± 2.0	0.7 ± 1.5	1.0 ± 1.4†	0.8 ± 1.1
CS(°)	−7.7 ± 2.4†	−4.9 ± 2.8	−0.7 ± 0.4	−0.9 ± 0.7	−1.0 ± 1.1	−0.1 ± 0.7	0.5 ± 0.8†	1.3 ± 0.9

*$P < 0.01$.
†$P < 0.05$.
AR indicates axial rotation; Cp LB, coupled lateral bending; Cp F/E, coupled flexion/extension; CS, cervical spondylosis.

deviations for range of motion to 1 side were computed in each group. Segmental motions were calculated as the average of the sum between left and right motions for coupled extension flexion, coupled anteroposterior translation, and coupled superoinferior translation, using constant codes between left and right rotation, and also calculated as the average difference between left and light motions for main axial rotation, coupled lateral bending, and lateral translation, using differing codes between left and right rotation.

In addition, degree of head rotation was measured accurately on the absolute spatial coordinate system using volume registration of the occiput. A 3D animation of each subject was also constructed to facilitate an understanding of these complex motions using methods that have been fully described in previous studies.[11–13]

Comparisons of rotations and translations by spinal level between groups were performed using the nonparametric Mann-Whitney *U* test. Values of $P < 0.05$ were considered statistically significant.

RESULTS

Mean (±standard deviation) maximal head rotation was 72.0 ± 5.3° in the control group and 63.4 ± 8.9° in the CS group. As a large range of mobility was identified between groups, only kinematics at 45° of head rotation was compared.

Main Axial Rotation at 45° Head Rotation

Significant decreases in axial rotation were observed at C5–C6 and C6–C7 in the CS group at both 45° (Table 1 and Figure 2).

Coupled Lateral Bending at 45° Head Rotation

In both groups, coupled lateral bending opposite to head rotation to 1 side was observed in the upper cervical spine, whereas the subaxial cervical spine displayed coupled lateral bending in the same direction as head rotation (Table 1 and Figure 3). Significant decreases in coupled lateral bending were observed at Oc–C1, C5–C6, and C6–C7, and significant increases were also observed at C1–C2, C2–C3, and C3–C4 in the CS group compared with the control group.

Coupled Flexion/Extension at 45° Head Rotation

In both groups, extension coupled with head rotation to 1 side occurred in the upper and middle cervical spine, whereas in the lower cervical spine, flexion was coupled with head rotation (Table 1 and Figure 4). Significant decreases in coupled flexion/extension were observed at C6–C7, and significant increases were observed at Oc–C1 in the CS group compared with the control group.

Coupled Translations at 45° Head Rotation

Although coupled translations were barely seen and most of these values were beyond the limit of accuracy and too small to analyze statistically, concerning lateral translation, the CS group showed a tendency toward larger motion in the middle

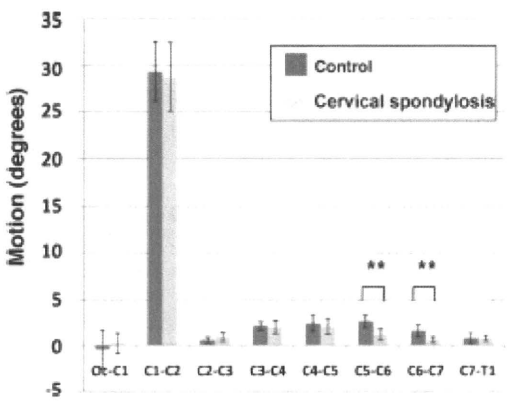

Figure 2. Main axial rotation by spinal level for the Control and CS groups at 45° head rotation. Data represent mean ± standard deviation. *$P < 0.05$ and **$P < 0.01$.

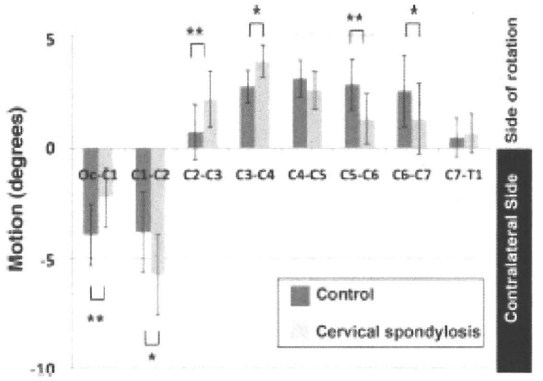

Figure 3. Coupled lateral bending by spinal level for the Control and CS groups at 45° head rotation. Data represent mean ± standard deviation. $^{*}P < 0.05$ and $^{**}P < 0.01$.

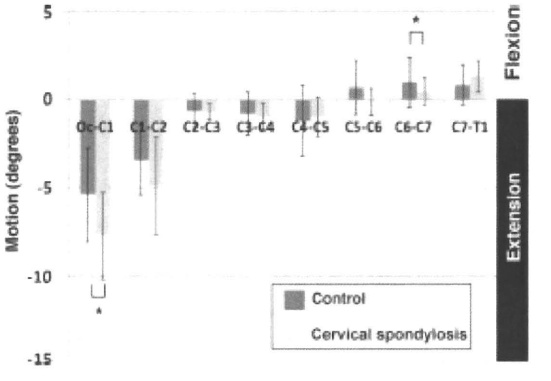

Figure 4. Coupled flexion/extension by spinal level for the Control and CS groups at 45° head rotation. Data represent mean ± standard deviation. $^{*}P < 0.05$ and $^{**}P < 0.01$.

cervical spine compared with the control group (Table 2 and Figure 5).

DISCUSSION

Hypomobility at the Lower Cervical Segments in the Degenerative Cervical Spine

General agreement is seen in the literature that the most commonly involved level is at C5–C6, followed by C6–C7 with increasing age.[4,15,16] Degenerative changes are speculated to arise most frequently at these levels because maximum distribution of axial load occurs at the lower cervical levels representing the sites of lordotic inversion.[10,17,18] To the best of our knowledge, few studies have addressed the *in vivo* kinematic changes of cervical motion segments after degeneration, despite a number of 2-dimensional flexion/extension motion studies of the normal cervical spine. Dvorak *et al*[4] showed significant hypomobility in sagittal rotation at C6–C7 in subjects with degenerative spine based on a functional flexion/extension radiographic study. Miyazaki *et al*[10] revealed that decreased segmental motion during extension-flexion starts at C4–C5 and C5–C6 with increasing age in a kinetic MRI study. No studies have clarified the kinematic changes occurring head rotation, because of the difficulties inherent in measuring such 3D motions *in vivo*. This study succeeded in detecting kinematics of the cervical spine during head rotation in patients with CS using a unique method. Comparison with healthy cervical spines yielded comparable results to previous cervical flexion/extension motion studies, showing significant decreases in main axial rotation and coupled lateral bending during headrotation at C5–C6 and C6–C7 segments in the CS group. These results indicate that in the lower cervical spine of the CS group, which is vulnerable to degeneration, motion segments might have already been in the stabilization phase put forward by Kirkaldy-Willis and Farfan[19] and hypomobility might have been present.

As for main axial motion, significant compensatory motions were barely seen at the suprajacent segments. However, the question arises as to where compensation occurs, because both groups were compared at 45° fixed head rotation. Total cervical motion at 45° fixed head rotation and the

TABLE 2. Coupled Translations by Spinal Level for Control and CS Groups at 45° Head Rotation

	C2–C3	C3–C4	C4–C5	C5–C6	C6–C7	C7–T1
Lateral translation						
Control (mm)	0.2 ± 0.0	−0.2 ± 0.0	−0.4 ± 0.1	−0.5 ± 0.0	−0.3 ± 0.1	−0.2 ± 0.0
CS (mm)	−0.2 ± 0.2	−0.6 ± 0.3	−0.5 ± 0.2	−0.5 ± 0.4	−0.3 ± 0.1	−0.2 ± 0.0
Superoinferior translation						
Control (mm)	−0.1 ± 0.1	−0.1 ± 0.2	−0.0 ± 0.3	0.1 ± 0.3	0.3 ± 0.3	0.2 ± 0.5
CS (mm)	−0.2 ± 0.1	−0.1 ± 0.2	−0.1 ± 0.1	−0.0 ± 0.1	0.1 ± 0.2	0.1 ± 0.2
Anteroposterior translation						
Control (mm)	−0.1 ± 0.2	−0.1 ± 0.2	−0.0 ± 0.3	0.2 ± 0.3	0.4 ± 0.4	0.3 ± 0.7
CS (mm)	−0.1 ± 0.1	−0.1 ± 0.2	−0.1 ± 0.2	0.1 ± 0.1	0.1 ± 0.1	0.2 ± 0.1

CS indicates cervical spondylosis.

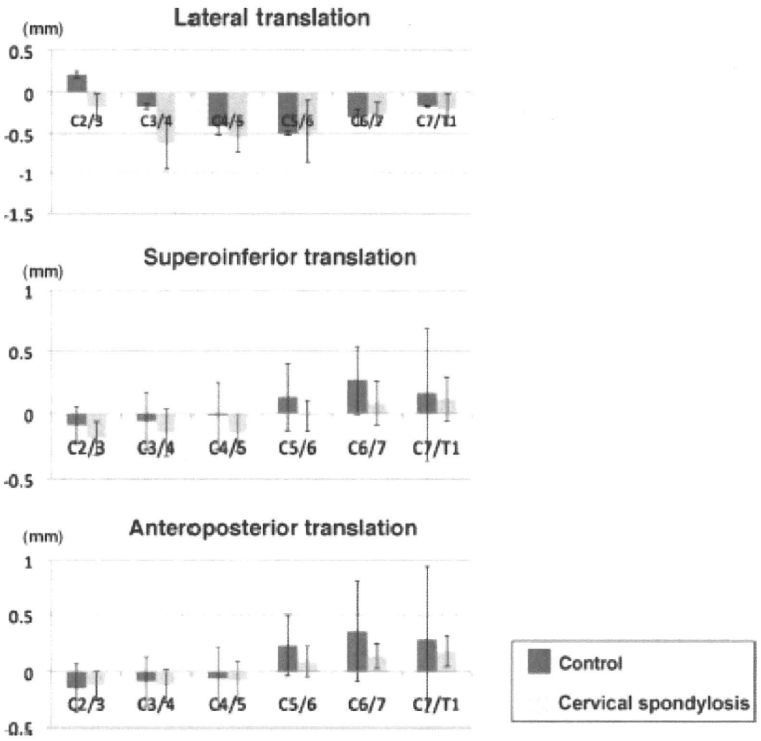

Figure 5. Coupled translations by spinal level for the Control and CS groups at 45°. Intervertebral motions are expressed in mm.

contribution ratio ([total cervical rotation [°]/head rotation [°]] × 100) was 38.9° (89%) in the control group and 36.4° (83%) in the CS group. Slight but significant decreases in motion were identified in the CS group ($P < 0.01$, nonparametric Mann-Whitney *U* test). Given the above findings, some compensation can safely be said to occur beyond the upper thoracic spine, but the precise location at which compensation occurred could not be identified.

Coupling Pattern of the Degenerative Cervical Spine

Although coupling patterns provide important clues for the detection of selected elements of spine pathology,[20] coupled motion is thought to be difficult to assess precisely because of the complex 3D motions and *in vivo* explorations have been rare. White and Panjabi[21] described abnormal coupled motion as 1 feature of abnormal spine kinematics. As we have already succeeded in accurately detecting 3D coupled motion of the cervical spine *in vivo*, we investigated coupled patterns of the spondylotic cervical spine during head rotation and compared the results with those of the healthy cervical spine. Although almost the same coupling patterns were identified in both groups, the spondylotic cervical spine showed significant hypomobility in axial and lateral directions at the lower cervical spine and significant lateral hypermobility, including coupled lateral bending at the middle cervical spine (Table 3). The fact that hypermobility in lateral directions was observed at the middle cervical spine in the CS group compared with the control group indicates that intervertebral mechanical stresses are increased in lateral directions at the middle cervical spine. As head axial rotation movements are reportedly half as frequent as flexion/extension movements and just as frequent as lateral bending movements,[22] head axial rotation movements are often repeated during ADL. Given these considerations, repetition of head rotation in ADL might have promoted degenerative changes of the middle cervical spine in the CS group.

This study has several limitations. First, the information was not obtained from true real-time imaging in the upright position. Second, the study was conducted using a small sample size. Third, patients were grouped together in the CS group despite a wide degree of variation in age, deformity, and symptoms. In this regard, further research focused more specifically on a particular subject group should be undertaken to elucidate details of the natural history of cervical

TABLE 3. Summary of Coupling Pattern for the CS Group Compared With the Control Group

	Main Motion	Coupled LB	Coupled F/E
Upper (Oc–C2)	N	N	N
Middle (C2–C5)	N	Increased	N
Lower (C5–T1)	Decreased	Decreased	N

LB indicates lateral bending; F/E, flexion/extension; N, no marked difference between groups; CS, cervical spondylosis.

spine motion after degeneration. Fourth, there might be some differences between the images obtained from the 2 different scanners in the 2 groups. Despite all these limitations, no other approaches to kinematic analysis have provided the kind of information given in this study, and these findings thus represent a step toward a better understanding of CS.

In conclusion, we accurately determined *in vivo* 3D kinematics of the spondylotic cervical spine during head rotation and compared the results with kinematics for the healthy cervical spine for the first time. Comparison with healthy cervical spine yielded comparable results with previous cervical flexion/extension motion studies, significant decreases in main axial rotation, and coupled lateral bending during head rotation at C5–C6 and C6–C7 segments in the spondylotic cervical spine. Although almost the same coupling patterns were observed in both groups, significant hypomobility in axial and lateral directions at the lower cervical spine and significant hypermobility in lateral directions at the middle cervical spine were apparent in the spondylotic cervical spine. Because hypermobility in lateral directions at the middle cervical spine in the CS group were thought to reflect increased intervertebral mechanical stresses, repeated head rotation in ADL might contribute to the progression of degenerative changes in the middle cervical vertebrae of the spondylotic cervical spine.

Key Points

- *In vivo* 3D kinematics of the spondylotic cervical spine during head rotation was investigated for the first time.
- Almost the same coupling patterns were observed in both healthy and spondylotic cervical spine.
- Significant hypomobility at the lower cervical segments were observed in the spondylotic cervical spine; significant decreases in main axial rotation and coupled lateral bending at C5–C6 and in coupled flexion/extension as well as main axial rotation and coupled lateral bending at C6–C7.
- On the contrary, significant hypermobility in lateral directions were observed at the middle cervical segments in the spondylotic cervical spine; significant increases in coupled lateral bending at C2–C3 and C3–C4.

Acknowledgments

The authors thank Ryoji Nakao and Aya Sasaki for assisting with software programming and Yoshihiro Sakaguchi for help with magnetic resonance imaging.

References

1. Garfin SR. Cervical degenerative disorders: etiology, presentation, and imaging studies. *Instr Course Lect* 2000;49:335–8.
2. Kolstad F, Myhr G, Kvistad KA, et al. Degeneration and height of cervical discs classified from MRI compared with precise height measurements from radiographs. *Eur J Radiol* 2005;55:415–20.
3. Muhle C, Metzner J, Weinert D, et al. Classification system based on kinematic MR imaging in cervical spondylitic myelopathy. *AJNR Am J Neuroradiol* 1998;19:1763–71.
4. Dvorak J, Panjabi M, Grob D, et al. Clinical validation of functional flexion/extension radiographs of the cervical spine. *Spine* 1993;18:120–7.
5. Holmes A, Wang C, Han ZH, et al. The range and nature of flexion-extension motion in the cervical spine. *Spine* 1994;19:2505–10.
6. Dai L. Disc degeneration and cervical instability. Correlation of magnetic resonance imaging with radiography. *Spine* 1998;23:1734–8.
7. Lind B, Sihlbom H, Nordwall A, et al. Normal range of motion of the cervical spine. *Arch Phys Med Rehabil* 1989;70:692–5.
8. Dvorak J, Antinnes JA, Panjabi M, et al. Age and gender related normal motion of the cervical spine. *Spine* 1992;17:S393–8.
9. Cheng JS, Liu F, Komistek RD, et al. Comparison of cervical spine kinematics using a fluoroscopic model for adjacent segment degeneration. Invited submission from the Joint Section on Disorders of the Spine and Peripheral Nerves, March 2007. *J Neurosurg Spine* 2007;7:509–13.
10. Miyazaki M, Hong SW, Yoon SH, et al. Kinematic analysis of the relationship between the grade of disc degeneration and motion unit of the cervical spine. *Spine* 2008;33:187–93.
11. Ishii T, Mukai Y, Hosono N, et al. Kinematics of the upper cervical spine in rotation: *in vivo* three-dimensional analysis. *Spine* 2004;29:E139–44.
12. Ishii T, Mukai Y, Hosono N, et al. Kinematics of the subaxial cervical spine in rotation *in vivo* three-dimensional analysis. *Spine* 2004;29:2826–31.
13. Ishii T, Mukai Y, Hosono N, et al. Kinematics of the cervical spine in lateral bending: *in vivo* three-dimensional analysis. *Spine* 2006;31:155–60.
14. Fujii R, Sakaura H, Mukai Y, et al. Kinematics of the lumbar spine in trunk rotation: *in vivo* three-dimensional analysis using magnetic resonance imaging. *Eur Spine J* 2007;16:1867–74.
15. Shedid D, Benzel EC. Cervical spondylosis anatomy: pathophysiology and biomechanics. *Neurosurgery* 2007;60:S7–13.
16. Friedenberg ZB, Edeiken J, Spencer HN, et al. Degenerative changes in the cervical spine. *J Bone Joint Surg Am* 1959;41:61–70.
17. Gallucci M, Limbuci N, Paonessa A, et al. Degenerative disease of the spine. *Neuroimaging Clin N Am* 2007;17:87–103.
18. Jager HJ, Gordon-Haris L, Mehring UM, et al. Degenerative change in the cervical spine and load-carrying on the head. *Skeletal Radiol* 1997;26: 475– 81.
19. Kirkaldy-Willis WH, Farfan HF. Instability of the lumbar spine. *Clin Orthop Relat Res* 1982;(165):110–23.
20. Cook C, Heqedus E, Showalter C, et al. Coupling behavior of the cervical spine: a systematic review of the literature. *J Manipulative Physiol Ther* 2006;29:570–5.
21. White AA, Panjabi MM. *Clinical Biomechanics of the Spine*. 2nd ed. Philadelphia, PA: Lippincott Williams & Wilkins; 1990.
22. Sterling AC, Cobian DG, Anderson PA, et al. Annual frequency and magnitude of neck motion in healthy individuals. *Spine* 2008;33:1882–8.